For submission to *Biochemical Pharmacology*

α-Elapitoxin-Aa2a, a long-chain snake α-neurotoxin with potent actions on muscle $(\alpha 1)_2\beta\gamma\delta$ nicotinic receptors, lacks the classical high affinity for neuronal α7 nicotinic receptors[#]

Benjamin Blacklow[a], Rachelle Kornhauser[b], Peter G Hains[c,f], Richard Loiacono[b], Pierre Escoubas[d,g], Andis Graudins[e,h], Graham M Nicholson[a,*].

[a] *Neurotoxin Research Group, Department of Medical & Molecular Biosciences, University of Technology, Sydney, P.O. Box 123, Broadway NSW 2007, Australia*

[b] *Department of Pharmacology, Monash University, Clayton VIC 3168, Australia*

[c] *Sydney Eye Hospital, University of Sydney, Sydney NSW 2007, Australia*

[d] *Institut de Pharmacologie Moléculaire et Cellulaire (IPMC), Université de Nice Sophia Antipolis, CNRS UMR6097, 660 Route des Lucioles, 06560 Valbonne, France*

[e] *Emergency Medicine, Prince of Wales Hospital, Randwick, 2031, Australia*

[f] *Present address: Cell Signalling Unit, Children's Medical Research Institute, Westmead NSW 2145, Australia*

[g] *Present address: VenomeTech, 473 Route des Dolines - Villa 3, Sophia Antipolis, 06560 Valbonne, France*

[h] *Present address: Southern Health Emergency Medicine Research Group, Southern Clinical School, Faculty of Medicine, Nursing and Health Sciences, Monash University, Clayton VIC, 3168, Australia.*

[#] *Ethical statement*: The authors declare that all animal experiments described in the paper comply with Australian animal ethics regulations.

* Corresponding author. Professor Graham Nicholson, PhD
Neurotoxin Research Group
Department of Medical & Molecular Biosciences
University of Technology, Sydney
PO Box 123

Broadway, NSW, 2007
Australia
Tel.: +61–2–9514–2230; fax: +61–2–9514–8206
E-mail address: Graham.Nicholson@uts.edu.au (G. Nicholson).

Abbreviations: ACh, acetylcholine; ANOVA, analysis of variance; CBCNM, chick biventer cervicis nerve-muscle; CCh, carbachol; ESI-QTOF, electrospray ionization quadrupole time-of-flight; MALDI-TOF, matrix-assisted laser desorption/ionization time-of-flight; nAChR, nicotinic acetylcholine receptor; NSW, New South Wales; EPTX, elapitoxin; RP-HPLC, reversed-phase high-pressure liquid chromatography; TFA, trifluoroacetic acid; t_{90}, time to 90% neuromuscular blockade; V_e, elution volume; V_o, void volume.

The N-terminal sequence of α-elapitoxin-Aa2a reported in this paper has been submitted to the UniProt Knowledgebase (http://www.uniprot.org/) under the UniProtKB/SwissProt accession code P86522 (NXLA2_ACAAN).

ABSTRACT

In contrast to all classical long-chain α-neurotoxins possessing the critical fifth disulfide bond, α-elapitoxin-Aa2a (α-EPTX-Aa2a), a novel long-chain α-neurotoxin from the common death adder *Acanthophis antarcticus*, lacks affinity for neuronal α7-type nicotinic acetylcholine receptors (nAChRs). α-EPTX-Aa2a (8850 Da; 0.1–1 μM) caused a concentration-dependent inhibition of indirect twitches, and blocked contractures to cholinergic agonists in the isolated chick biventer cervicis nerve-muscle preparation, consistent with a postsynaptic curaremimetic mode of action. α-EPTX-Aa2a (1–10 nM) produced a potent pseudo-irreversible antagonism of chick muscle nAChRs, with an estimated pA_2 value of 8.311 ± 0.031, which was not reversed by monovalent death adder antivenom. This is only 2.5-fold less potent than the prototypical long-chain α-neurotoxin, α-bungarotoxin. In contrast, α-EPTX-Aa2a produced complete, but weak, inhibition of ^{125}I-α-bungarotoxin binding to rat hippocampal α7 nAChRs (pK_I = 3.670), despite high sequence homology and similar mass to a wide range of long-chain α-neurotoxins. The mostly likely cause for the loss of α7 binding affinity is a leucine substitution, in loop II of α-EPTX-Aa2a, for the highly conserved Arg^{33} in long-chain α-neurotoxins. Arg^{33} has been shown to be critical for both neuronal and muscle activity. Despite this substitution, α-EPTX-Aa2a retains high affinity for muscle $(\alpha1)_2\beta\gamma\delta$ nAChRs. This is probably as a result of an Arg^{29} residue, previously shown to be critical for muscle $(\alpha1)_2\beta\gamma\delta$ nAChR affinity, and highly conserved across all short-chain, but not long-chain, α-neurotoxins. α-EPTX-Aa2a therefore represents a novel atypical long-chain α-neurotoxin that includes a fifth disulfide but exhibits differential affinity for nAChR subtypes.

Keywords: Snake toxin; long-chain α-neurotoxin; α-elapitoxin-Aa2a; *Acanthophis antarcticus*; neuronal α7 receptor

1. Introduction

Monomeric postsynaptic snake α-neurotoxins, from the venom of elapid and hydrophiid snakes, produce rapid paralysis of skeletal muscle by a potent curaremimetic action to antagonise nicotinic acetylcholine receptors (nAChR). Snake α-neurotoxins and other animal toxins have therefore been fundamental tools for studying nAChR structure and function. Indeed certain conopeptide nAChR antagonists from *Conus* spp. are currently in development as potential analgesic agents [1].

All nAChRs are composed of five subunits, with muscle-type receptors consisting of four subunits: $(\alpha 1)_2\beta\gamma\delta$ in the developing muscle, and $(\alpha 1)_2\beta\varepsilon\delta$ in the mature human form [2]. The most widely studied muscle-type nAChR, however, is the heteropentameric $(\alpha 1)_2\beta\gamma\delta$ receptor expressed in the electric organ from various species of *Torpedo* [3]. Much of the progress in nAChR research was originally connected to the accessibility of high quantities of this muscle-type nAChR. Nevertheless, it was the discovery, and subsequent use, of polypeptide elapid snake α-neurotoxins as potent and selective receptor ligands that made possible the purification of preparative amounts of *Torpedo* nAChR. Thus snake α-neurotoxins were, and remain, invaluable tools for the purification and more recently characterization of nAChR receptors. In addtion to their use as tools, such post-synaptic nAChRs inhibitors may also find use as therapeutic agents, in pathologies involving dysfunction of the neuromuscular junction.

The polypeptide backbone of all snake α-neurotoxins adopts the same overall tertiary fold. This comprises four conserved disulfide bridges, forming a hydrophobic core, and three adjacent loops (I, II and III) rich in β-pleated sheets; hence their alternate name 'three-fingered' neurotoxins [4]. Snake α-neurotoxins are divided into two groups based on the length of their primary sequence: short-chain *vs*. long-chain α-neurotoxins. Short-chain α-neurotoxins typically comprise of 60–62 amino acids with four disulfide bonds, while long-chain α-neurotoxins typically consist of 66–75 residues with an additional C-terminal tail segment, a slightly shorter first loop, and normally five disulfide bonds [4]. The additional fifth disulfide bond (Cys^{IV}–Cys^{V}) in long-chain α-neurotoxins cyclizes a helix-like conformation at the tip of the middle loop (loop II) [4]. Despite these structural variations, snake α-neurotoxins from both groups bind to similar sites, and with comparable high affinity, on *Torpedo* or skeletal muscle nAChRs (Table 1). Nevertheless, a major difference is that short-chain α-neurotoxins are known to associate 6–7-fold faster to, and dissociate 5–9-fold more rapidly from, skeletal muscle nAChRs than long-chain α-neurotoxins [5]. Indeed, the slowed dissociation rate can be the result of pseudo-irreversible binding [6].

More recently it was found that long-chain α-neurotoxins, and the structurally related, but dimeric, κ-bungarotoxin (from *Bungarus multicinctus*), also antagonize neuronal nAChRs,

while short-chain α-neurotoxins that lack this fifth disulfide bridge bind to neuronal nAChRs with around 3–5 orders of magnitude lower affinity (see Table 1). In contrast to muscle-type $(\alpha1)_2\beta\gamma\delta$ receptors, neuronal nAChRs consist of only one or two subunits: α (α2-α10) and β (β2-β4). They can be homopentameric (eg. neuronal α7-type or $(\alpha7)_5$) or heteropentameric (eg. ganglionic α3β2-type or $(\alpha3)_2(\beta2)_3$) in configuration. Studies have revealed that long-chain α-neurotoxins potently block neuronal homopentameric nAChRs, especially the α7-type [7]. Several lines of evidence have suggested that high affinity for the α7 nAChR is associated with the presence of the extra fifth disulfide (Cys^{IV}–Cys^{V}) in loop II of long-chain α-neurotoxins. Firstly, selective reduction and carboxymethylation of the fifth disulfide of the long-chain α-cobratoxin resulted in a marked reduction in neuronal α7 nAChR binding affinity. Importantly however there was no significant change in the affinity of the alkylated toxin for the muscle $(\alpha1)_2\beta\gamma\delta$ nAChR [7]. In parallel experiments, mutation of each of the half-cystines into serine in the fifth disulfide of α-cobratoxin or α-bungarotoxin, also resulted in loss of affinity for the α7 nAChR but maintained high affinity for $(\alpha1)_2\beta\gamma\delta$ nAChRs [8-10]. Secondly, the removal of the fifth disulfide bond Cys^{27}–Cys^{31} in the structurally related κ-bungarotoxin, selective for α3β2 neuronal nAChRs, also resulted in a significant loss of affinity despite maintenance of the β-sheet structure in this region [11]. Lastly, Lc long neurotoxin 1 from *Laticauda colubrina*, despite showing high sequence homology with other long-chain α-neurotoxins, lacks the fifth disulfide bond and lacks affinity for the α7 nAChR (Table 1 and [7]). The above evidence clearly supports the hypothesis that the fifth disulfide is critical for neuronal nAChR affinity [7-11]. To further test this hypothesis Lyukmanova et al. [12] inserted the cyclized loop formed by the fifth disulfide (Cys^{27}–Ser^{33}) in loop II from long-chain *Naja oxiana* neurotoxin I (NTI) into the homologous position (Ser^{29}–His^{31}) of short-chain *N. oxiana* neurotoxin II (NTII). Importantly, five of the six functionally important residues, with the exception of Phe^{65} in the C-terminal tail, are found in loop II. The resultant NTII/I chimera caused a potent inhibition of human α7 nAChR (IC_{50} 6.1 nM), comparable to the native long-chain NTI (IC_{50} 34 nM). This further indicates the importance of this region for nAChR subtype selectivity.

A large number of studies have identified a variety of snake α-neurotoxins subtypes from marine and Asian terrestrial elapids (Serpentes, Elapidae), however only more recently have toxins of Australo-Papuan terrestrial elapids begun to be characterized pharmacologically. Amongst these snakes, the Australian common death adder (*Acanthophis antarcticus*) has a highly lethal venom, with an LD_{50} in mice of 0.338 mg/kg [13] and an average venom yield of 79.1 mg, equivalent to more than 11,000 LD_{50} doses in mice [14]. Despite its viper-like appearance, *A. antarcticus* venom lacks cytotoxins and myotoxins [15-17] but has recently been shown to express a presynaptic neurotoxin complex [18], often associated with

Australian elapid venoms. Furthermore several short-chain [19, 20] and long-chain [21-23] α-neurotoxins have been identified in the venom of *A. antarcticus*, consistent with the venom of other elapids, although pharmacological characterization remains mostly incomplete. Indeed, the toxicity of all these toxins, except the long-chain α-neurotoxin acanthophin d [22], is assumed based on size of toxin and symptoms arising from single parenteral administration in mice. As such there has been no thorough testing to determine the mode of action for these neurotoxins.

In the present study we describe the isolation and characterization of a novel long-chain postsynaptic α-neurotoxin from *A. antarcticus* (NSW) venom. We have named the novel toxin α-elapitoxin-Aa2a (α-EPTX-Aa2a) as recommended by the rational nomenclature system proposed for the naming of spider, *Conus* and other peptide toxins [24]. The activity descriptor prefix 'α' indicates an antagonist of nicotinic acetylcholine receptors, 'elapitoxin' is the generic name for toxins from the family Elapidae (see Table 3 in the Supplementary data within [24]), 'Aa' is the genus and species descriptor for *Acanthophis antarcticus*, '2' represents long-chain α-neurotoxins ('1' represents short-chain α-neurotoxins, '3' represents neuronal κ-neurotoxins), and 'a' denotes the first paralog (isoform) found.

We demonstrate using a variety of nerve-muscle organ bath functional assays and competition receptor binding assays that α-EPTX-Aa2a shows high affinity for muscle-type $(\alpha 1)_2\beta\gamma\delta$ nAChR. However, unlike other long-chain α-neurotoxins, α-EPTX-Aa2a has very weak activity on neuronal α7 nAChR, despite the presence of a fifth disulfide bond.

2. Materials and methods

2.1. Venom / toxin preparation and storage

Lyophilized *A. antarcticus* venom (New South Wales variant) was provided by the Australian Reptile Park (Gosford, NSW). Death adders were collected from their natural habitats in the Sydney metropolitan region. To minimise the effects of individual variations in venom [25], venom was collected from several snakes, pooled and lyophilized by the supplier. Venom obtained from a single individual female snake (Bega, NSW) was also provided by the Australian Reptile Park. Venom and isolated toxins were stored lyophilized at –20 °C until required.

2.2. Venom fractionation

Bioassay-guided isolation of toxins from whole venom was performed using a Shimadzu CLASS-VP HPLC system. Prior to separation, samples were suspended in equilibration buffer and centrifuged at 10,000 rpm for 5 min (MiniSpin plus centrifuge; Eppendorf, North

Ryde, NSW, Australia), with the resulting supernatant applied to the HPLC system. Elution profiles were then monitored at 280 and 214 nm.

2.2.1. Size-exclusion FPLC

Whole venom was applied to a Superdex-75 FPLC column (10 x 300 mm, 13 µm; GE Healthcare, Sydney, NSW, Australia) previously equilibrated with ammonium acetate (0.1 M, pH 6.8). Fractions were then eluted using an isocratic gradient of ammonium acetate at a flow rate of 0.75 ml/min. Resulting fractions were screened for neurotoxic and myotoxic activity using the isolated chick biventer cervicis nerve-muscle (CBCNM) preparation (see section 2.5). The approximate molecular mass estimation for each eluted fraction was achieved by calibrating the size-exclusion FPLC column using a series of molecular weight markers, as previously described [26].

2.2.2. Ion-exchange FPLC

Neurotoxic components, identified following isolation of whole venom using size-exclusion FPLC, were further purified using cation-exchange FPLC. Samples were applied to a TOSOH TSK-GEL SP-5PW cation-exchange column (7.5 x 75 mm, 10 µm; SUPELCO, Bellefonte, PA, USA) with fractions eluted using an ammonium acetate gradient (Buffer A: H_2O, pH 6.8; Buffer B: 1 M ammonium acetate, pH 6.8; Gradient: 0-10 min, 2% B; 10-55 min, 2-98% B) at a flow rate of 0.75 ml/min. Resulting fractions were again tested for toxicity and phospholipase A_2 (PLA_2) activity.

2.2.3. Reversed-phase HPLC

Ion-exchange FPLC fractions retaining neurotoxic activity were further purified using reversed-phase HPLC (RP-HPLC). Ion-exchange fractions were applied to a Vydac C8 RP-HPLC column (4.6 x 250 mm, 5 µm; Grace, Deerfield, IL, USA) with fractions eluted using an acetonitrile/trifluoroacetic acid (TFA) gradient (Buffer A: 0.1% v/v TFA, Buffer B: acetonitrile / 0.085% v/v TFA; Gradient, 0-10 min, 2% B; 10-50 min, 2-98% B) at a flow rate of 0.75 ml/min.

2.3 Bicinchoninic Acid Protein (BCA) Assay:

Following lyophilisation, the protein concentrations of purified proteins were determined using the Quantipro™ BCA assay kit (Sigma-Aldrich). Protein contents between 5–200 µg/ml were detected at 560 nm by a Titertek Multiscan Plus MKII (type 313) plate reader (Flow Laboratories Australasia, North Ryde, NSW, Australia). A standard curve was created using bovine serum albumin from which protein concentrations of the venom fractions were

interpolated. Yields were then expressed as a percentage of whole venom loaded onto the column (3 mg).

2.4. Mass determination of purified samples

2.4.1. Matrix-assisted laser desorption/ionization time-of-flight (MALDI-TOF) mass spectrometry

Lyophilized RP-HPLC samples were analyzed to determine mass and confirm purity using a Shimadzu AXIMA TOF^2 (Shimadzu Oceania, Rydalmere, NSW, Australia), as previously described [18].

2.4.2. Electrospray-ionization quadrupole time-of-flight (ESI-QTOF) mass spectrometry

Once purity was confirmed, the definitive masses of RP-HPLC samples were determined using a QSTAR Elite hybrid QTOF mass spectrometer system (Applied Biosystems/MDS Sciex, Foster City, CA, USA) equipped with a nanospray source, as previously described [18].

2.5. Isolated chick biventer cervicis nerve-muscle preparation

Isolated peptide fractions were tested for neurotoxic and myotoxic activity using the isolated CBCNM preparation [27]. Male Australorps chicks aged 1–7 days were anesthetized with CO_2 and exsanguinated in accordance with Institutional Animal Care & Ethics Committee approval conforming to the Australian NHMRC Code of Practice for the use of animals in research. The biventer-cervicis muscle with attached nerve was dissected and placed in an organ bath (8 ml) under 1 gram of resting tension. The organ bath contained Krebs-Henseleit solution of the following composition (in mM): NaCl, 118.4; KCl, 4.7; $MgSO_4$, 1.2; KH_2PO_4, 1.2; $NaHCO_3$, 25.0; D-glucose, 11.1; and $CaCl_2$, 2.5, which was bubbled with carbogen (95% O_2 and 5% CO_2) and maintained at 34 °C. Indirect nerve stimulation was applied to the motor nerve with a Grass S88 stimulator using supramaximal 30 V square-wave pulses of 0.2 ms duration at 0.1 Hz. Contractions were measured using an isometric force transducer (ADInstruments, Belle Vista, NSW, Australia). The nerve-evoked muscle twitch contractions were allowed to equilibrate for 30 minutes. Exclusive electrical stimulation of the nerve was ensured by complete blockade of twitches using 10 μM *d*-tubocurarine. Washout was then repeated until twitch tension returned to its original amplitude. Contractions to various exogenous agonists were recorded in the absence of electrical stimulation before, and after, incubation with toxin. The final bath concentration and period of incubation was as follows: acetylcholine (ACh, 1 mM) for 30 s; carbachol (CCh, 20 μM) for 60 s; KCl (40 mM) for 30 s. After each agonist incubation period, washout was repeated until a stable baseline was observed. Following addition of toxin, twitch height was monitored for up to 5 hours, or until

twitches were abolished. Time-matched controls confirmed that muscle fatigue was not significant up to 5 hours after introduction into the organ bath. Muscle tension from each force transducer was fed through a ML221 bridge amp (ADInstruments) and recorded using a Powerlab 2/25 system (ADInstruments) connected to a Macintosh computer. Data were digitized at 140 Hz, modified with a 50 Hz mains filter and a 20–200 Hz low pass filter. Muscle tension was recorded using CHART v5.5.4 software (ADInstruments). Twitch tension and contractile responses to exogenous agonists were expressed as a percentage of the initial control twitch contraction amplitude prior to addition of toxin.

2.5.1. Antivenom reversibility studies

The efficacy of monovalent death adder antivenom (CSL Biotherapies, Melbourne, Australia) to neutralise the activity of purified α-EPTX-Aa2a was assessed by preincubating the organ bath with 5 U/ml of antivenom for 10 min prior to addition of toxin. Reversibility studies were also performed by the addition of 5 U/ml monovalent death adder antivenom at 90% inhibition of twitch contractions (t_{90}). Twitches were monitored for 5 hours after addition of α-EPTX-Aa2a or until stable twitch height was reached.

2.5.2. Carbachol concentration-response curves

Cumulative concentration-response curves to carbachol (CCh) were obtained in the unstimulated chick biventer cervicis nerve-muscle preparation. Concentration-response curves were constructed from successive additions of CCh without washout, at final bath concentrations of 0.8–1000 μM prior to, and following, a 1 hour incubation with toxin. Successive doses of CCh were added only after stable muscle tension was achieved following the previous dose. If no immediate increase in muscle tension was visible, additional doses were added after a 3 minute waiting period.

2.6. Membrane preparation for radioligand binding assays

Receptor-enriched membranes were prepared according to a method adapted from Whiteaker et al. [28]. Eight female Sprague-Dawley (180–220 g) rats were gassed by CO_2 (80% in 20% O_2) and killed by decapitation. The brains were removed and placed on an ice-cold platform. The hippocampus from each brain was dissected and homogenized using a glass homogeniser in 50 volumes of ice-cold hypotonic homogenizing buffer of the following composition (in mM): NaCl, 14.4; KCl, 0.2; $CaCl_2$, 0.2; $MgSO_4$, 0.1; HEPES 2; pH 7.5. Membrane fractions were collected by centrifugation at 25,000 *g* for 15 min at 4 °C. The pellets were then resuspended in fresh homogenization buffer, incubated on ice for 10 min then harvested by centrifugation as before. Each pellet was washed twice more by re-

suspension / centrifugation before storage at –80 ºC until required. Protein content was then quantified using a BCA protein assay (see section 2.3).

2.7 ^{125}I-α-Bungarotoxin binding assay

Competition binding studies using ^{125}I-α-bungarotoxin (Perkin Elmer, Waltham, MA, USA) were adapted from Davies et al. [29]. Brain membrane pellets were resuspended to a concentration of 2 mg/ml in binding buffer of the following composition (in mM): NaCl, 144; KCl, 1.5; $CaCl_2$, 2; $MgSO_4$, 1; Tris-HCl, 200; HEPES, 20; bovine serum albumin, 0.1% (w/v); pH 7.5. Membrane protein samples were pipetted into 96-well plates and incubated for 5 hr in a 100 µl final buffer volume containing 1 nM ^{125}I-α-bungarotoxin and increasing concentrations of α-EPTX-Aa2a, or the positive control *d*-tubocurarine. Total binding was determined in the absence of any displacing toxin. Non-specific binding was determined in the presence of 1 mM nicotine. Specific binding was defined as the difference between total and non-specific binding. All samples were in triplicate. The incubations were terminated by harvesting membranes onto polyethyleneimine soaked (0.5% w/v, for 2 h) GF/C filters (UniFilter-96, Perkin Elmer) using a Tomtec 96 Harvester Mach III M (Tomtec, USA). Subsequently, filters were washed three times with ice-cold binding buffer. Filters were then dried overnight and counted on a Perkin Elmer Wallac Wizard 1470 Automatic Gamma Counter (Perkin Elmer).

2.8. Secretory phospholipase A_2 ($sPLA_2$) activity assay

The $sPLA_2$ activity of whole venom and isolated toxins were determined using a colorimetric $sPLA_2$ assay kit (Cayman Chemical Ltd, Ann Arbor, MI, USA) as previously described [18]. $sPLA_2$ activity was calculated as micromoles of substrate hydrolyzed per minute per milligram of enzyme (µmol/min/mg), using bee venom (*Apis mellifera*) as a positive control.

2.9. Partial N-terminal sequence determination

Partial N-terminal sequencing of purified proteins was performed by the Biomolecular Research Facility at the University of Newcastle, NSW, Australia using an Applied Biosystems Procise HT Protein Sequencer. Samples were loaded onto a biobrene-treated, precycled disc and subjected to N-terminal (Edman) sequencing. Sequence homology of purified proteins with existing toxins was determined using a Blastp search of the UniProt Knowledgebase (http://ca.expasy.org/tools/blast) followed by a ClustalW multiple alignment.

2.10. Chemicals and drugs

Unless otherwise stated, all chemicals and drugs were purchased from Sigma-Aldrich, Castle Hill, NSW, Australia. Unless otherwise indicated, all drugs were made up and diluted in distilled water.

2.11. Data analysis

Biventer cervicis muscle twitch contraction amplitude was expressed as a percentage of initial amplitude, prior to addition of α-EPTX-Aa2a. Contractile responses to exogenous cholinergic agonists and KCl were expressed as a percentage of their amplitude prior to addition of α-EPTX-Aa2a. To compare neurotoxicity, the time taken to produce 90% inhibition of nerve-mediated twitch contractions (t_{90}) was determined as a quantitative measure of potency. Values for t_{90} were calculated for each experiment by determining the elapsed time after toxin addition at 10% of the initial twitch contraction amplitude, and then the means and standard error of the means (SEM) were calculated. Statistical analyses and non-linear curve-fitting were performed using the PRISM 5.0 software package (GraphPad Software, San Diego, CA, USA). Using PRISM, cumulative CCh concentration–response curves in the absence, and presence, of α-EPTX-Aa2a were fitted via nonlinear regression to the following four-parameter logistic function:

$$y = \mathrm{A} + \frac{E_{\max} - \mathrm{A}}{1 + 10^{(\log EC_{50} - \log[\mathrm{CCh}])^{n_H}}} \qquad (1)$$

where A and E_{max} denote the lower and upper asymptotes, respectively, log[CCh] the logarithm of the carbachol concentration, n_H the midpoint slope (Hill coefficient), and $\log EC_{50}$ the logarithm of the midpoint location parameter. To determine antagonist potency the negative logarithm of EC_{30} values (pEC_{30} values) interpolated from Eq. (1) were fitted to the following modified Lew Angus equation [30, 31]:

$$\mathrm{pEC}_{30} = -\log([B]^s + 10^{-\mathrm{p}K}) - \log c \qquad (2)$$

where pEC_{30} denotes the negative logarithm of the EC_{30}, [*B*] denotes the antagonist concentration, p*K* and log *c* are fitting constants, and *s* is equivalent to the Schild slope factor [32]. When concentration-response curve spacings deviate from the predictions of a simple competitive interaction *s* is significantly different from unity and the pA_2 value can be estimated by $pA_2 = pK / s$. Deviation from competitive antagonism was also confirmed by comparing the goodness-of-fit of Eq. (2) with a simple Lew Angus equation (Eq. 3) using an extra sum-of-squares *F* test within the PRISM software package [33].

$$pEC_{30} = -\log([B] + 10^{-pK_B}) - \log c \qquad (3)$$

where the pK_B is given directly as a fitted parameter [30, 31].

^{125}I-α-Bungarotoxin competition binding curves were fitted to Hill equation via non-linear regression in order to derive estimates of the IC_{50} (median inhibitory concentration):

$$y = \frac{100}{1 + 10^{(\log IC_{50} - x)n_H}} \qquad (4)$$

where, x is the logarithm of the antagonist concentration, n_H the midpoint slope (Hill coefficient), and $\log IC_{50}$ the logarithm of the midpoint location parameter. Competition binding data were fitted to both one-site and two-site binding models, and the best fit determined by an extra sum-of-squares *F* test using PRISM. IC_{50} values were converted to K_I values (competitor–receptor dissociation equilibrium constant) according to the following equation [34]:

$$K_I = \frac{IC_{50}}{1 + \left(\frac{[D]}{K_D}\right)} \qquad (5)$$

where [*D*] and K_D denote the concentration and dissociation constant, respectively, of ^{125}I-α-bungarotoxin. The K_D of α-bungarotoxin was previously determined to be 0.91 nM [29] for determining K_I values and [*D*] was 1 nM. Statistical significance of CCh concentration-response data was confirmed using a one-way analysis of variance (ANOVA) with repeated measures, followed by a Bonferroni-corrected multiple *t*-test. Significant changes in responses to exogenous cholinergic agonists and KCl were confirmed with a Student's paired *t*-test. A *p*-value of 0.05 was employed for all statistical analyses. Unless otherwise stated, data are expressed as mean ± SEM.

3. Results

3.1. Venom fractionation

Isolation of toxins from snake venom sourced from an individual snake benefits from ease of purification, as a result of a reduction in the complexity of peptide/protein components. However it may not be representative of all venoms from that species. Thus the presence of purified toxin from individual snake venom was also confirmed in the pooled venom sample.

Separation of *A. antarcticus* whole venom by size-exclusion FPLC produced a characteristic pattern of fractions from both pooled and individual venom samples (Fig. 1A and B, respectively). Under non-reducing conditions, fractionation of pooled or individual *A. antarcticus* venom produced a characteristic pattern of seven peaks. This was similar to that observed with other geographic variants of *A. antarcticus* and certain other Australo-Papuan species of *Acanthophis* [26]. The retention time of the main fraction (*f*3) was 17.5–22.1 min and displayed rapid and potent neurotoxicity as evidenced by a rapid inhibition of twitch tension (see section 3.3). *f*3 had an estimated component mass range of *ca*. 3.8–17.7 kDa (note: minimum marker mass is 6.5 kDa) following calibration of the size-exclusion column with a series of molecular weight markers (Fig. 1C and D). Peak absorbances of pooled and individual venom occurred at 19.6 and 19.1 min, respectively (Fig. 1A and B), corresponding to a molecular mass of *ca*. 8.7 kDa (Fig. 2A) and *ca*. 10.3 kDa (Fig. 2B). *f*3 therefore is likely to contain Kunitz-type protease inhibitors (*ca*. 6400–6700 Da), short-chain α-neurotoxins (*ca*. 6700–7100 Da), long-chain α-neurotoxins (*ca*. 7200–8900 Da) and monomeric PLA_2 neurotoxins (*ca*. 12800–14000 Da).

Fraction 3 from both pooled and individual venoms was further separated using cation exchange FPLC (Fig. 1E and F, respectively), with the fraction exhibiting the largest yield (*f*3.11 in pooled venom, 58.8–61.3 %B; *f*3.7 in individual venom, 58.8–64.0 %B) being selected for further separation using C8 RP-HPLC. This produced five major peaks in both pooled and individual venom samples (Fig. 1G and H, respectively). Of these five peaks the second (*f*3.11.2, 45.0–46.1 %B; *f*3.7.2, 43.8–45.4 %B), third (*f*3.11.3, 47.0–49.1 %B; *f*3.7.3, 51.3–53.3 %B) and fifth fraction (*f*3.11.5, 47.7–49.1 %B; *f*3.7.5, 51.0–53.0 %B) in both venom samples were selected for further analysis as they possessed the highest yields. Only the second fractions (*f*3.11.2 and *f*3.7.2) in each respective venom were found to be pure and possessed strong neurotoxic activity (see section 3.3). Fraction 3.7.2 represents *ca*. 3% of individual snake venom and while *f*3.11.2 corresponded to *ca*. 1% of pooled snake venom, confirmed by both area under the curve and dry weight. Following subsequent biochemical characterization and neurotoxicity testing (see below), the toxin present in both these fractions was found to be identical and was named α-elapitoxin-Aa2a (α-EPTX-Aa2a).

3.2. Mass spectrometry

MALDI-TOF mass spectrometry confirmed the purity of *f*3.11.2 (data not shown) and *f*3.7.2 (Fig. 2A). ESI-QTOF mass spectrometry determined the definitive mass of *f*3.11.2 (data not shown) and *f*3.7.2 (Fig. 2B) to both be 8850.0 Da, confirming their matching identity. This mass is consistent with long-chain snake α-neurotoxins although, to our knowledge it is the highest mass elapid snake α-neurotoxin so far described.

3.3. Neurotoxicity studies

Given that *f*3.7.2 was less easily contaminated by closely eluting fractions, and more abundant, all subsequent biochemical and pharmacological characterization was performed with α-EPTX-Aa2a derived from individual venom (*f*3.7.2). α-EPTX-Aa2a (0.1–1 μM) produced a rapid concentration-dependent inhibition of nerve-evoked twitch contractions in the CBCNM preparation, while time-matched controls were not significantly inhibited (Fig. 3Aa-Ab). The t_{90} value of 1 μM α-EPTX-Aa2a for inhibition of twitch contractions was 15.5 ± 3.2 min (n = 4) that increased to 38.5 ± 6.6 min using 100 nM (n = 4; Fig. 3Ad). Importantly, following complete neuromuscular blockade with α-EPTX-Aa2a responses to the exogenous cholinergic agonists ACh and CCh were completely abolished ($p < 0.001$, one-way ANOVA, n = 4; Fig. 3Ba-Bb). Conversely, slow muscle fibre contractures to the depolarizing agonist KCl were not significantly inhibited ($p > 0.05$, one-way ANOVA, n = 4; Fig. 3Ba-Bb). Furthermore, α-EPTX-Aa2a failed to induce any significant change in baseline tension (data not shown). These actions are consistent with the presence of a snake α-neurotoxin that inhibits postsynaptic nAChRs without any overt signs of myotoxicity.

3.4. Antivenom neutralization and reversibility studies

Preincubation with monovalent death adder antivenom (5 U/ml) was completely effective in preventing the development of neuromuscular blockade (Fig. 3Ac), and inhibition of responses to cholinergic agonists (Fig. 3Bb; n = 4, one-way ANOVA, $p > 0.05$ *vs*. time-matched controls), by 0.1 μM α-EPTX-Aa2a. However, attempts at reversing neuromuscular blockade by 0.1 μM α-EPTX-Aa2a using monovalent death antivenom (5 U/ml) applied at t_{90} failed to reverse toxicity (Fig. 4A-B). Significant inhibition of contractures to ACh and CCh were also still observed after incubation with antivenom at t_{90} (Fig. 4C; n = 4, one-way ANOVA, $p < 0.001$ *vs*. time-matched controls).

3.5. Secretory phospholipase A_2 ($sPLA_2$) activity

The $sPLA_2$ activity of whole venom and α-EPTX-Aa2a was 257 ± 14 μmol/min/mg and 0.4 ± 0.6 μmol/min/mg, respectively (n = 4, data not shown). In comparison, the $sPLA_2$ activity of the positive control, *Apis mellifera* bee venom, was 287 ± 10 μmol/min/mg (n = 18).

3.6. Effects on carbachol concentration-response curves

Cumulative CCh concentration-response curves in the CBCNM preparation in the absence, and presence, of α-EPTX-Aa2a resulted in a decrease in the maximal response to CCh, consistent with pseudo-irreversible binding to the muscle nAChR. To measure the antagonist

(α-EPTX-Aa2a) potency, the antagonist dissociation constant (K_B) or pA_2 would normally be determined by Schild regression analysis [32], based on the comparison of equieffective agonist concentrations. However, α-EPTX-Aa2a caused a concentration-dependent decrease in the maximum CCh response (E_{max}) in the CBCNM preparation (n = 4–6; one-way ANOVA, $p < 0.05$; Fig. 5A). Since it is not possible to compare EC_{50} values under conditions where maximal responses fall below the EC_{50}, traditional Schild plot analysis could not be performed. Hence the pA_2 value of α-EPTX-Aa2a was determined using the modified Lew Angus method (Eq. 2) However, the normal dependent variable (i.e. pEC_{50}) in the equations was replaced with pEC_{30} (i.e. equieffective agonist concentrations based on the level representing the 30% maximal response of the control CCh concentration–response curve) as described in Christopoulos et al. [30, 31]. This was necessary since it is not possible to compare EC_{50} values under conditions of varying maximal responses. This violates the null-method approach of traditional Schild plot analysis, which assumes that the EC_{50} values being compared represent equieffective concentrations. Following an F-test, the data were best fitted by a 'modified Lew Angus' equation (Eq. 2; $p = 0.0253$, $F_{1,2} = 38.11$), rather than a 'simple Lew Angus' equation (Eq. 3), producing an estimated pA_2 value for α-EPTX-Aa2a of 8.311 ± 0.031 (Fig. 5B and C).

3.7. Effects on neuronal nicotinic receptors (nAChRs)

In hippocampus homogenate, the positive control *d*-tubocurarine was a potent inhibitor of specific radioiodinated α-bungarotoxin binding to rat neuronal α7 nAChRs, however α-EPTX-Aa2a only inhibited ^{125}I-α-bungarotoxin binding at much higher concentrations. Following an F-test, the competition binding data were best fitted by a single-site binding model (Eq. 4) rather than a two-site model (*d*-tubocurarine, $p = 0.3520$, $F_{4,15} = 1.198$; α-EPTX-Aa2a, $p = 0.9491$, $F_{4,13} = 0.1716$). Using Eq. 5, *d*-tubocurarine and α-EPTX-Aa2a were found to have K_I values of 4.07 ± 2.99 μM and 214 ± 134 μM, respectively (n = 3; Fig. 5D).

3.8. N-terminal sequence

A 35 residue partial N-terminal sequence was determined for α-EPTX-Aa2a by Edman degradation (Fig. 6). The α-EPTX-Aa2a sequence was subjected to a Blastp analysis of the UniProt Knowledgebase and found to show high homology with a range of long-chain snake α-neurotoxins from *A. antarcticus*. To avoid the confusing *ad hoc* naming system for snake toxins we have elected to employ the recently proposed rational nomenclature system for peptide toxins [24]. Accordingly, the *A. antarcticus* toxins with high homology to α-EPTX-Aa2a were the paralogs α-EPTX-Aa2e (formerly Aa e [23]; 8752 Da, 83% homology), α-EPTX-Aa2b (formerly Aa b [21]; 8135 Da, 80% homology), and α-EPTX-Aa2d (formerly

acanthophin d [22]; 8387 Da, 80% homology), but not the short-chain α-neurotoxins α-EPTX-Aa1a (formerly acanthophin a, [20]; *ca*. 7700 Da) and α-EPTX-Aa1c (formerly Aa c, [19]; 6880 Da).

4. Discussion

Previous *in vitro* studies from our laboratories have shown that Australo-Papuan death adder (*Acanthophis* spp.) venoms are among the most neurotoxic elapid venoms [35, 36]. While we have recently characterized the presence of a presynaptic $sPLA_2$ neurotoxin complex in *Acanthophis antarcticus* venom [18, 26], the slow development of neurotoxicity by presynaptic neurotoxins cannot explain the rapid neurotoxicity seen with whole venom [37]. It is commonly regarded that this rapid neurotoxicity is mainly postsynaptic in origin with five curaremimetic α-neurotoxins previously isolated. However, none of these toxins have been pharmacologically characterised, particularly their actions on nAChR subtypes.

In the present study, α-elapitoxin-Aa2a was isolated as a single peak by successive size-exclusion, cation-exchange and reversed-phase HPLC separation. Its presence was confirmed within pooled and individual *A. antarcticus* (NSW variant) venom, representing a minor fraction of both individual and pooled venom samples (3% and 1%, respectively). The definitive mass of α-EPTX-Aa2a was determined by ESI-QTOF mass spectrometry to be 8850.0 Da, which is consistent with the mass of previously isolated long-chain α-neurotoxins from *A. antarcticus*, including: α-EPTX-Aa2b (8135 Da; [21]), α-EPTX-Aa2d (8387 Da; [22]) and both isoforms of α-EPTX-Aa2e (8752 Da; [23]). Despite the confirmed presence of α-EPTX-Aa2a in both individual and pooled venom samples by MALDI-TOF mass spectrometry, a component of this mass was not previously observed in LC/ESI-MS fingerprinting of whole *A. antarcticus* (NSW) pooled venom [38]. This may reflect the problem of ion suppression of protein mixtures using electrospray mass spectrometry methods.

The N-terminal sequence, mass and cysteine spacing of α-EPTX-Aa2a indicates that this toxin is a classical three-fingered neurotoxin, and has only limited sequence homology to non-conventional ('weak') snake toxins, such as irditoxin, denmotoxin and α-colubritoxin, and short-chain α-neurotoxins [4]. In particular, it lacks the extended loop I and the associated functionally important residues, characteristic of short-chain α-neurotoxins such as erabutoxin a. Furthermore, the fifth disulfide is not located in loop I (N-terminus loop), characteristic of 'weak' or non-conventional toxins (see Fig. 7).

Given the high sequence homology and mass consistent with other elapid postsynaptic neurotoxins, and the previous lack of pharmacological characterization of homologous toxins from *A. antarcticus* venom, α-EPTX-Aa2a was subjected to *in vitro* neurotoxicity testing using the CBCNM preparation. Initial *in vitro* testing confirmed the neurotoxic activity of α-EPTX-

Aa2a, presenting a rapid block of indirect twitch contractions and a block of contractures to exogenous cholinergic agonists, but not KCl. This indicates a postsynaptic neurotoxicity to block muscle $(\alpha1)_2\beta\gamma\delta$ nAChRs, in the absence of overt myotoxicity. Further cumulative CCh concentration-response curves in the CBCNM preparation in the presence of α-EPTX-Aa2a resulted in a decrease in the maximal response to CCh. This is consistent with pseudo-irreversible binding to the muscle nAChR, characterized by slow dissociation of the ligand from the receptor [6]. This pseudo-irreversible binding has been previously observed with certain elapid and colubrid short-chain, but more commonly long-chain, α-neurotoxins [5, 39-44]. Since it is not possible to compare EC_{50} values under conditions where maximal responses fall below the EC_{50}, traditional Schild plot analysis could not be performed. Hence the pA_2 value of α-EPTX-Aa2a was determined using the modified Lew Angus method using pEC_{30} values as described by Christopoulos et al. [30, 31] The Lew Angus method is considered to be a more accurate method for determining the potency of an antagonist than Schild plot analysis [33]. Using the modified Lew Angus equation, α-EPTX-Aa2a displayed significant binding affinity for the muscle $(\alpha1)_2\beta\gamma\delta$ nAChR with a pA_2 value of 8.311 ± 0.031, which is 107-fold more potent than *d*-tubocurarine (pA_2 = 6.28 ± 0.07; [43]). Moreover, it is only approximately 2.5-fold less potent than α-bungarotoxin (pA_2 = 8.71 ± 0.06) and comparable in potency to acantoxin IVa from *Acanthophis* sp. Seram (pA_2 = 8.36 ± 0.17; [43]). Along with the presynaptic $sPLA_2$ neurotoxin complex P-EPTX-Aa1a [18] and three other long-chain α-neurotoxins, α-EPTX-Aa2a may contribute to the difficulty in treating patients presenting late post-envenomation [45]. This may be the consequence of the high affinity for skeletal muscle nAChRs and slow dissociation as a result of pseudo-irreversible binding.

To investigate selectivity for other nAChR subtypes, the affinity of α-EPTX-Aa2a for homomeric α7 neuronal nAChR were studied in hippocampus homogenate, previously shown to be rich in this nAChR subtype [28]. Five other heteromeric nAChRs, containing various combinations of α3, α4, and/or α5 with β2 or β4 subunits, are also found in the hippocampus, however, snake neurotoxins lack affinity for these neuronal nAChR [46]. As expected the positive control, *d*-tubocurarine, was a potent inhibitor of ^{125}I-α-bungarotoxin binding to α7 nAChRs (K_i 4.07 ± 2.99 μM). In contrast to other long-chain α-neurotoxins, however, α-EPTX-Aa2a displayed the lowest affinity for α7 nAChRs of any long-chain α-neurotoxin, so far tested, with a K_i value of 214 ± 134 μM. This is about 165,000-fold less potent than α-bungarotoxin [43], and around 53-fold less potent than *d*-tubocurarine. Thus despite its mass and sequence identity with long-chain α-neurotoxins, α-EPTX-Aa2a displays very high selectivity for muscle $(\alpha1)_2\beta\gamma\delta$ nAChR in a similar fashion to short-chain α-neurotoxins, with whom it shares only limited sequence homology. Similar to short-chain

neurotoxins, α-EPTX-Aa2a shows approximately 44,000-fold selectivity for muscle $(\alpha1)_2\beta\gamma\delta$ *vs*. neuronal α7 receptors while long-chain α-neurotoxins have high affinity for α7 nAChR and only display 1–30-fold selectivity for muscle $(\alpha1)_2\beta\gamma\delta$ nAChRs (see Table 1).

Other long-chain α-neurotoxins are missing the fifth disulfide bond and have shown to lack affinity for neuronal α7 receptors. For example, the 69-residue toxin Lc long neurotoxin 1 from *Laticauda colubrina* consists of 69 residues with Asp^{30} and Gly^{34} replacing the usual cysteine residues yet only has a K_I of 7 μM for α7 nAChRs [7] (Table 1). Nevertheless, the N-terminal sequence of α-EPTX-Aa2a confirms the presence of the Cys^{IV}–Cys^{V} residues, necessary for the formation of the fifth disulfide bond. Therefore, it is likely that the limited number of amino acid substitutions in loop II of α-EPTX-Aa2a may be responsible for the loss of affinity for α7 nAChRs.

Using site-directed mutagenesis, a number of residues have previously been identified to be functionally important and form the bioactive surface of short-chain α-neurotoxins (erabutoxin a) and long-chain α-neurotoxins (α-cobratoxin). These 'pharmacophore' residues that interact with *Torpedo* $(\alpha1)_2\beta\gamma\delta$ nAChRs are identical in both toxins, and are located at homologous positions in loop II. The 'muscle' pharmacophore comprises, respectively, Lys^{27}/Lys^{23}, Trp^{29}/Trp^{25}, Asp^{31}/Asp^{27}, Phe^{32}/Phe^{29}, Arg^{33}/Arg^{33}, and Lys^{47}/Lys^{49} [10, 47-50]. Further studies have also identified that Trp^{25}, Asp^{27}, Phe^{29}, Arg^{33}, Arg^{36}, and Phe^{65} are also important in targeting α-cobratoxin to both neuronal α7 and muscle $(\alpha1)_2\beta\gamma\delta$ nAChRs, although Arg^{36} and Phe^{65} contribute more to the binding to α7 nAChRs. In addition to this common pharmacophore, Ala^{28}, Cys^{26}–Cys^{30}, and Lys^{35} provide additional bioactive surface 'neuronal' pharmacophore residues that interact specifically with α7 AChRs [10, 47]. Thus, apart from Phe^{65} in α-cobratoxin, all key residues important for neuronal α7 affinity in long-chain α-neurotoxins are located in loop II, including the fifth disulphide.

α-EPTX-Aa2a is therefore atypical in that it represents the first long-chain α-neurotoxin that includes a fifth disulfide but lacks affinity for the α7 neuronal nAChR. Clearly, therefore, the fifth disulfide is not the sole requisite for neuronal activity and non-conservative substitutions of other residues in the vicinity of the fifth disulfide bond must be directly related to the capacity of long-chain α-neurotoxins to recognize the neuronal α7 receptor. Importantly, in the neuronal pharmacophore region of loop II, there are only two non-conserved substitutions in α-EPTX-Aa2a. The mostly likely cause for the loss of affinity for the α7 receptor is the hydrophobic Leu^{33} substitution for the basic Arg^{33}, critical for both neuronal *and* muscle activity [7]. A similar hydrophobic isoleucine residue is usually present in short-chain α-neurotoxins (see Fig. 7). Interestingly, there is still very high affinity for muscle $(\alpha1)_2\beta\gamma\delta$ nAChRs, despite substitution of the critical Arg^{33} present in α-cobratoxin,

and highly conserved in all long-chain α-neurotoxins. Most likely retention of the high affinity for skeletal muscle $(\alpha1)_2\beta\gamma\delta$ receptors is due to the substitution of the aromatic Phe[29] normally present in long-chain α-neurotoxins for the critical Arg[29] in loop II of α-EPTX-Aa2a, although this remains to be confirmed experimentally. The corresponding Arg[33] in erabutoxin a has previously been shown to be critical for muscle affinity in short-chain α-neurotoxins, and is highly conserved across all short-chain α-neurotoxins. Nevertheless, downstream sequence variations may also be present such as a potential substitution for the critical Phe[65], further contributing to the loss of affinity. At present it is also unknown if α-EPTX-Aa2a differentially interacts with adult $(\alpha1)_2\beta\varepsilon\delta$ and embryonic $(\alpha1)_2\beta\gamma\delta$ AChRs of mammalian skeletal muscle.

The above evidence indicates the commonly accepted dogma, that all long-chain α-neurotoxins with a fifth disulfide block neuronal α7 nAChRs, appears to be overstated. Some 'classical' long-chain α-neurotoxins may lack affinity for the neuronal α7 nAChR. Caution should therefore be exercised if pharmacological characterization has not been performed on long-chain α-neurotoxins as the present study would suggest that not all long-chain toxins have affinity for neuronal α7 nAChR. Three other long-chain α-neurotoxins share the R33L and F29R substitution in the loop II 'neuronal pharmacophore' region: EPTX-Aa2e (formerly Aa e), α-EPTX-As2a (formerly long neurotoxin 2 from *Austrelaps superbus*) and α-EPTX-Al2a (formerly long neurotoxin from *Austrelaps labialis*). Although pharmacological characterization of these toxins remains incomplete, we would predict that these toxins would also lack affinity for neuronal α7 nAChR (see Fig. 6). Current work aims to confirm this hypothesis.

In conclusion, α-EPTX-Aa2a represents the first long-chain α-neurotoxin isolated from *A. antarcticus* to be fully pharmacologically characterised, and reveals an unique atypical selectivity for muscle *vs*. neuronal nAChRs not previously reported for long-chain α-neurotoxins. α-EPTX-Aa2a together with Lc long neurotoxin 1 from *Laticauda colubrina* [7] that lacks the fifth disulfide, behave functionally as short-chain neurotoxins at α7 nAChRs, despite their classification as long-chain α-neurotoxins. Thus, functional classification of α-neurotoxins requires pharmacological characterization of toxins at both skeletal muscle and neuronal nAChRs, rather than assumption of nAChR subtype activity based on size and number of disulfide bonds.

Acknowledgements

This work was supported in part by an Australian Postgraduate Award to BB, a DEST-ISL grant (FR050106 to GMN) and a CNRS PICS grant (3603 to PE). The authors would like to thank Dr Matt Padula (University of Technology, Sydney) for assistance with ESI-QTOF mass spectrometry and Dr Sanjaya Kuruppu (Monash University) for assistance with pA_2 determinations.

Figures

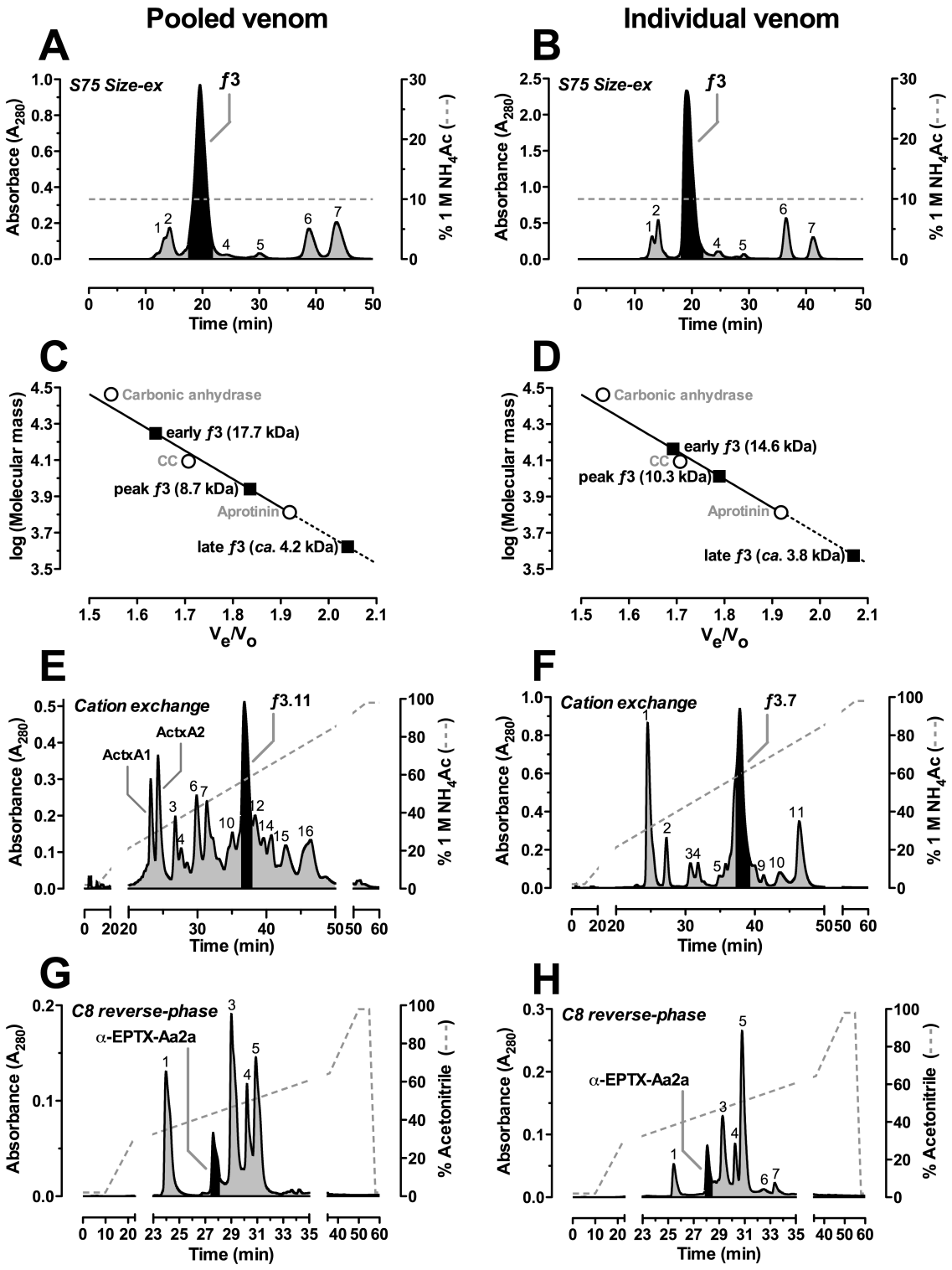

Fig. 1. Bioassay-guided isolation and purification of α-EPTX-Aa2a by liquid chromatography. The left-hand column shows successive separation of pooled *A. antarcticus* venom, while the right-hand column shows separation of venom milked from an individual female snake. (A-B) Representative size-exclusion FPLC chromatogram of *Acanthophis antarcticus* (NSW

variant) venom under non-reducing conditions with an isocratic flow of 0.1 M ammonium acetate pH 6.8 (grey dotted line) at 0.75 ml/min. Elution of proteins was monitored at 280 nm. (C-D) Calibration curve for the size-exclusion Superdex G-75 column using a series of molecular weight standards (open circles). For clarity bovine serum albumin (65 kDa) data is not shown, while 'CC' represents cytochrome c. The molecular mass of fraction *ƒ*3 (closed squares), containing α-EPTX-Aa2a, was determined to be *ca*. 4–18 kDa. The dotted line represents an extrapolation of masses below the mass of aprotinin (6.5 kDa). (E-F) The shaded fraction (*ƒ*3), containing α-EPTX-Aa2a, was collected for further purification via cation exchange FPLC with a gradient of 20–980 mM ammonium acetate pH 6.8 (grey dotted line) at 0.75 ml/min. (G-H) Final purification of α-EPTX-Aa2a from *ƒ*3.11 and *ƒ*3.7 using C8 reversed-phase HPLC employing an acetonitrile/TFA gradient (grey dotted line) at 0.75 ml/min. The resulting single protein peaks were named α-EPTX-Aa2a. For clarity the *x*-axis is split in panels E-H.

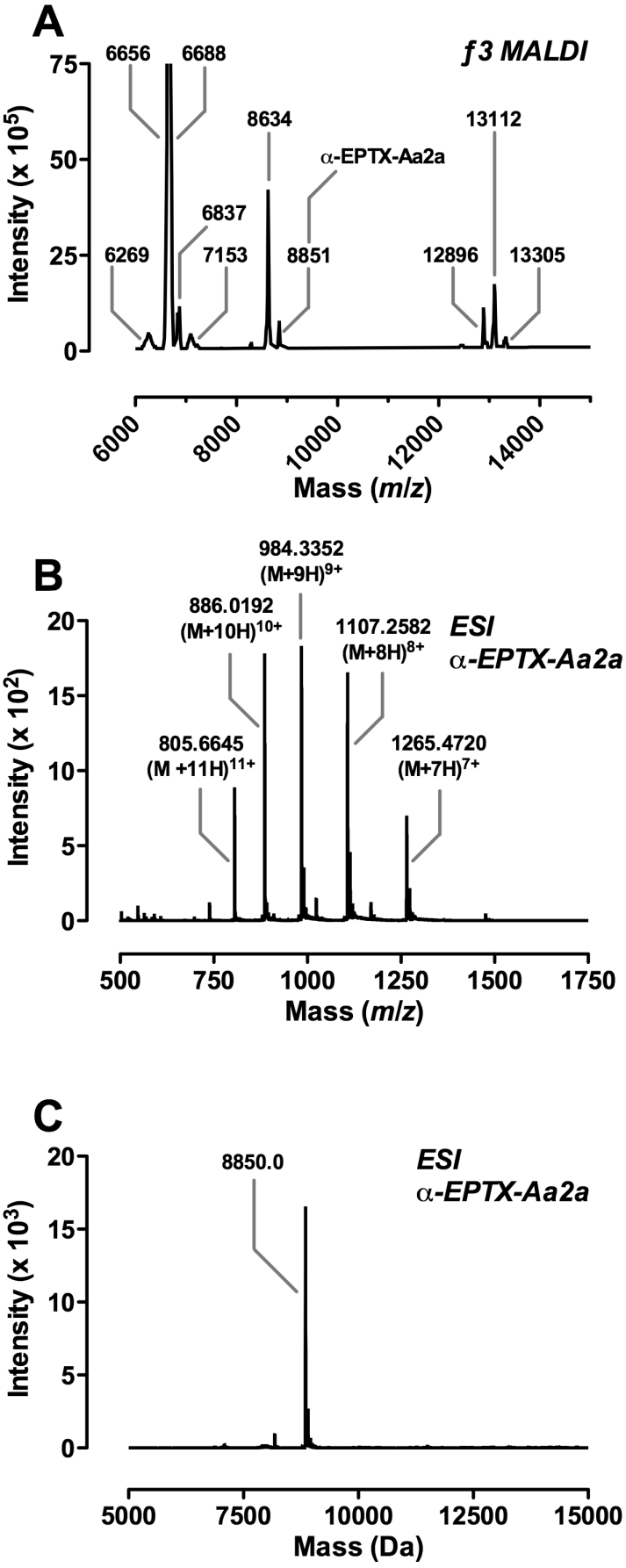
A
f3 MALDI
6656
6688
8634
13112
α-EPTX-Aa2a
6837
6269
7153
8851
12896
13305
Intensity (x 10^5)
75
50
25
0
6000
8000
10000
12000
14000
Mass (m/z)
B
984.3352
(M+9H)^9+
886.0192
(M+10H)^10+
1107.2582
(M+8H)^8+
ESI
α-EPTX-Aa2a
805.6645
(M +11H)^11+
1265.4720
(M+7H)^7+
Intensity (x 10^2)
20
15
10
5
0
500
750
1000
1250
1500
1750
Mass (m/z)
C
8850.0
ESI
α-EPTX-Aa2a
Intensity (x 10^3)
20
15
10
5
0
5000
7500
10000
12500
15000
Mass (Da)

Fig. 2. Mass spectrometry of α-EPTX-Aa2a isolated from individual female NSW *A. antarcticus* venom. (A) MALDI-TOF mass spectrum of *ƒ*3 focused on masses consistent with the presence of Kunitz-type protease inhibitors ('KPI', white boxed area, 6400–6700 *m*/*z*), short-chain α-neurotoxins ('Short', light gray, 6700–7100 *m*/*z*), long-chain α-neurotoxins ('Long', dark gray, 7200–8900 *m*/*z*) and monomeric $sPLA_2$ neurotoxins (PLA_2, black, 12800–14000 *m*/*z*), with α-EPTX-Aa2a (8851 *m*/*z*) highlighted. (B-C) ESI-QTOF mass spectrometry of α-EPTX-Aa2a showing (B) observed ion series and respective charge states for α-EPTX-Aa2a and (C) deconvoluted monoisotopic mass.

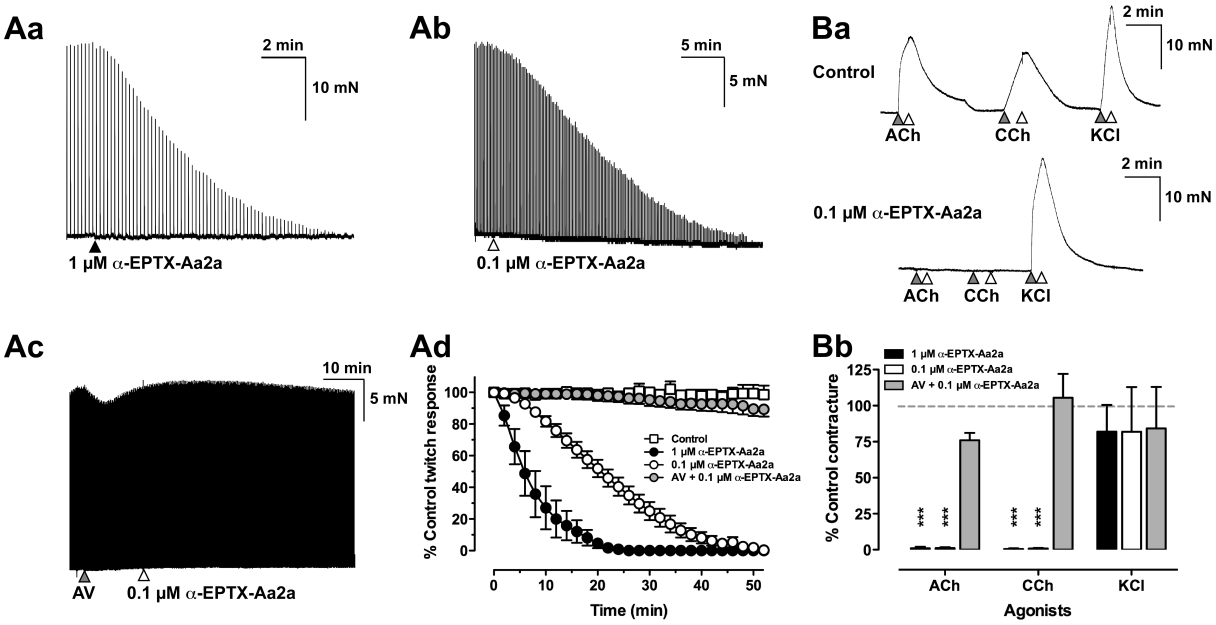

Fig. 3. Effects of α-EPTX-Aa2a on neuromuscular transmission in the CBCNM preparation. (A) Typical effects of α-EPTX-Aa2a on indirectly-stimulated (nerve-evoked) fast twitch contractions. (Aa-Ac) Representative traces showing rapid inhibition of twitch tension following application of 1 μM (Aa) and 0.1 μM (Ab) α-EPTX-Aa2a, and addition of 5 U/ml monovalent death adder antivenom 10 min prior to application of 0.1 μM α-EPTX-Aa2a (Ac). (Ad) Timecourse of inhibition of twitch contractions by 1 μM (closed circles, *n* = 4) and 0.1 μM (open circles, *n* = 4) α-EPTX-Aa2a in comparison to time-matched controls (open squares, *n* = 3). Addition of 5 U/ml monovalent death adder antivenom 10 min prior to application of 0.1 μM α-EPTX-Aa2a successfully prevented onset of toxicity (gray circles, *n* = 4). (Ba) Typical effect of 0.1 μM α-EPTX-Aa2a on slow fibre contracture responses to ACh, CCh and KCl prior to (upper trace), and following (lower trace), incubation with 0.1 μM α-EPTX-Aa2a. Markers beneath each trace indicate the bath application of either 1 μM ACh, 4 nM hPK1, or 50 mM KCl (grey arrowheads) or washout with Krebs solution (white arrowheads). (Bb) Data shows the percentage of control slow fibre contracture responses to exogenous agonists after complete inhibition of twitch contractions by 1 μM (closed bars, *n* = 4) and 0.1 μM (gray bars, *n* = 4) α-EPTX-Aa2a. In the case of 5 U/ml antivenom preincubated 10 min prior to addition of 0.1 μM α-EPTX-Aa2a data was recorded at 60 min. Note that α-EPTX-Aa2a completely inhibited responses to ACh and CCh. Data represent the mean ± SEM. ****p* < 0.001, significantly different from control response, one-way ANOVA.

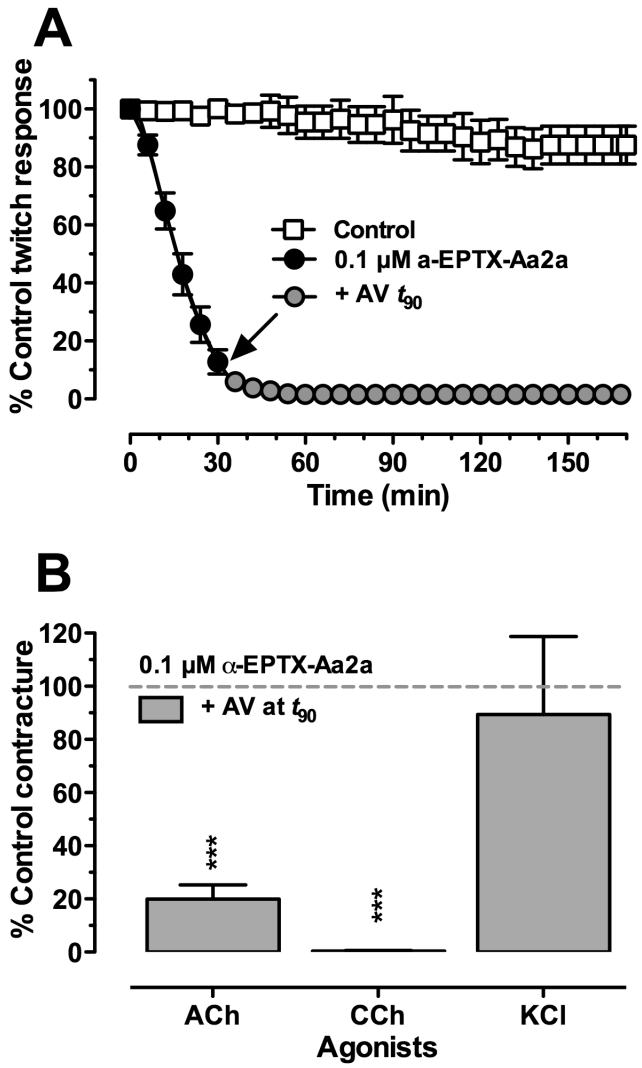

Fig. 4. Lack of reversibility of α-EPTX-Aa2a neurotoxicity by antivenom in the CBCNM preparation. (A) Representative trace showing inhibition of indirectly-stimulated (nerve-evoked) fast twitches following application of 0.1 µM α-EPTX-Aa2a and subsequent addition of 5 U/ml monovalent death adder antivenom at t_{90}. (B) Addition of 5 U/ml monovalent death adder antivenom at t_{90} (gray circles, n = 4), failed to reverse the inhibition of twitch contractions following incubation with 0.1 µM α-EPTX-Aa2a (closed circles). Time-matched controls are shown as open squares (n = 3). The arrow indicates the time of application of antivenom. For clarity, only data points recorded every 6 min are displayed. (C) Effects of antivenom on α-EPTX-Aa2a-induced block of ACh and CCh responses. Data was recorded at 60 min after attempts to reverse inhibition of α-EPTX-Aa2a by 5 U/ml monovalent death adder antivenom applied at t_{90} (open bars, n = 4). Data represent the mean ± SEM. ***p < 0.001; significantly different from control response, one-way ANOVA (n = 4).

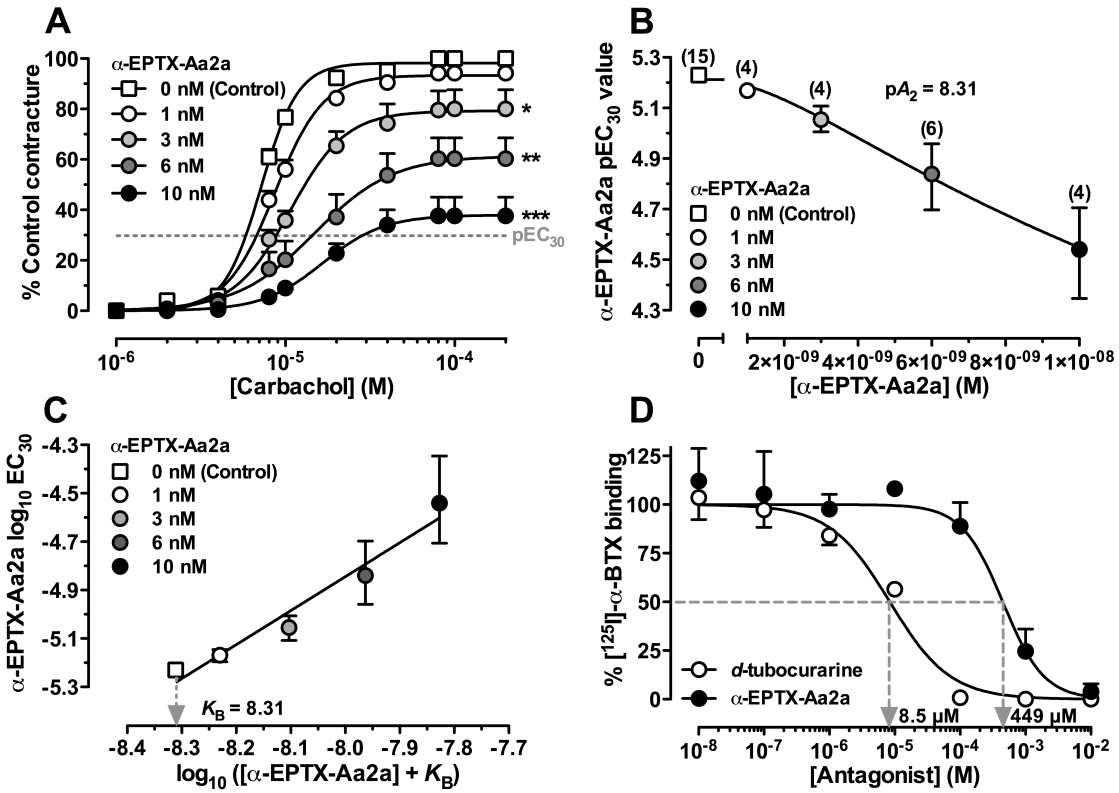

Fig. 5. Affinity of α-EPTX-Aa2a for chick muscle $(\alpha1)_2\beta\gamma\delta$ and rat brain α7 nAChRs. (A) Pseudo-irreversible inhibition of CCh concentration-response curve in the CBCNM preparation by increasing doses of α-EPTX-Aa2a. Data were fitted to a sigmoidal concentration-response curve (Eq. 1). * $p < 0.05$ *vs*. control, ** $p < 0.01$ *vs*. control, *** $p < 0.001$ *vs*. control. The grey dotted line indicates the pEC_{30} level used for calculations in panels B and C. (B) The pA_2 value for α-EPTX-Aa2a was calculated to be 8.311 ± 0.031 using a modified Lew Angus equation (Eq. 2). Number of experiments (*n*) are shown in brackets above each data point. Error bars represent the 95% confidence intervals. (C) Clark plot showing the effect of α-EPTX-Aa2a on CCh pEC_{30}. Data were fitted by linear regression. Error bars represent the 95% confidence intervals. (D) Inhibition of ^{125}I-α-bungarotoxin binding to rat brain neuronal α7 receptors by increasing concentrations of *d*-tubocurarine or α-EPTX-Aa2a (*n* = 3). Arrows indicate the IC_{50} values for the two antagonists. Data was fitted to the Hill equation (Eq. 4).

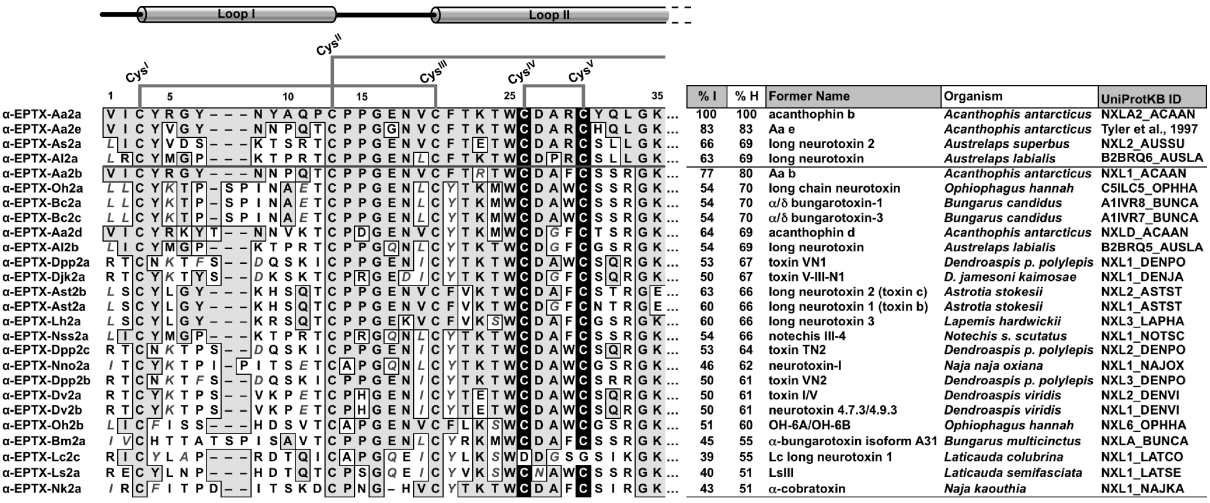

Fig. 6. Comparison of the partial N-terminal sequence of α-EPTX-Aa2a with other long-chain snake α-neurotoxins. Identical residues are in gray boxes while conservatively substituted resides are shown in gray italic text. Percentage identity (%I) is relative to α-EPTX-Aa2a while percentage homology (%H) includes conservatively substituted residues. The highly conserved disulfide bonding pattern, apart from α-EPTX-Lc2a, is shown above the sequences. Cysteine residues involved in the fifth disulfide (Cys^{IV}–Cys^{V}) are highlighted in black. 'UniProtKB ID' indicates the UniProt Knowledgebase ID code or source reference. 'Organism' refers to the venom source.

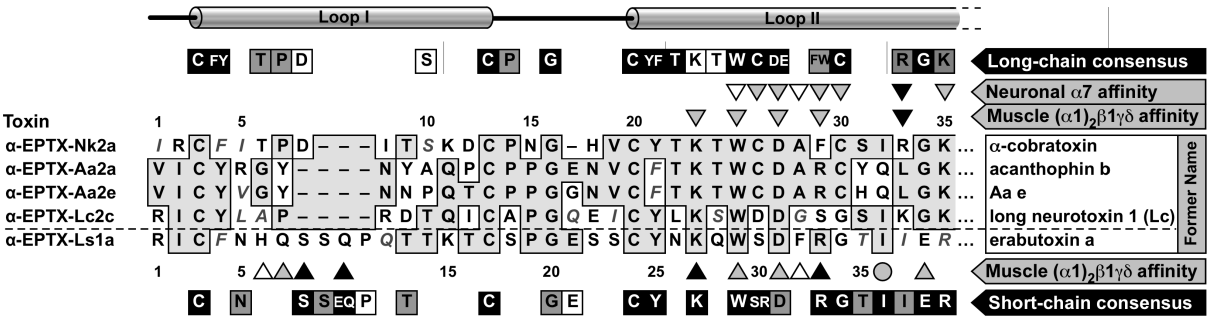

Fig. 7. Comparison of the sequence of α-EPTX-Aa2a with the pharmacophores of long-chain and short-chain α-neurotoxins. Long-chain α-neurotoxins (α-EPTX-Xx2x) are listed above the dotted line and the short-chain α-neurotoxin, α-EPTX-Ls1a (formerly erabutoxin a), below the dotted line. Consensus residues for long-chain (top) and short-chain (bottom) α-neurotoxins were taken from 30 representative sequences and are coded as 100% identity (black squares), 90-99% identity (grey) or 80-89% identity (white). Residues in α-cobratoxin and erabutoxin a whose mutation affects affinity for neuronal α7 (α-cobratoxin) and muscle-type $(\alpha1)_2\beta\gamma\delta$ (α-cobratoxin and erabutoxin a) nAChRs are marked with shaded arrowheads. Arrowheads identify residues whose mutation results in a decrease in affinity of between 5-

and 9-fold (white), a 10- and 100-fold decrease (gray), or >100-fold (black), while the gray circle indicates a mutation inducing an increase in affinity.

References from Table: please ignore
This study
[7, 43, 51]
[7, 43, 51]
[52]
[7, 53]
[7, 54]
[7]
[7]
[43]
[7, 55]
[7, 49]
[7, 49]
[41]
[56]
[40]
[7, 57, 58]
[59]
[60]

References

[1] Clark RJ, Jensen J, Nevin ST, Callaghan BP, Adams DJ, Craik DJ. The engineering of an orally active conotoxin for the treatment of neuropathic pain. Angew Chem Int Ed Engl 2010;In press.

[2] Mishina M, Takai T, Imoto K, Noda M, Takahashi T, Numa S, et al. Molecular distinction between fetal and adult forms of muscle acetylcholine receptor. Nature 1986;321:406-11.

[3] Unwin N. Refined structure of the nicotinic acetylcholine receptor at 4Å resolution. J Mol Biol 2005;346:967-89.

[4] Tsetlin V, Utkin Y, Kasheverov I. Polypeptide and peptide toxins, magnifying lenses for binding sites in nicotinic acetylcholine receptors. Biochem Pharmacol 2009;78:720-31.

[5] Chicheportiche R, Vincent JP, Kopeyan C, Schweitz H, Lazdunski M. Structure-function relationship in the binding of snake neurotoxins to the *Torpedo* membrane receptor. Biochemistry 1975;14:2081-91.

[6] Lew MJ, Ziogas J, Christopoulos A. Dynamic mechanisms of non-classical antagonism by competitive AT_1 receptor antagonists. Trends Pharmacol Sci 2000;21:376-81.

[7] Servent D, Winckler-Dietrich V, Hu HY, Kessler P, Drevet P, Bertrand D, et al. Only snake curaremimetic toxins with a fifth disulfide bond have high affinity for the neuronal α7 nicotinic receptor. J Biol Chem 1997;272:24279-86.

[8] Servent D, Mourier G, Antil S, Ménez A. How do snake curaremimetic toxins discriminate between nicotinic acetylcholine receptor subtypes. Toxicol Lett 1998;102-103:199-203.

[9] Servent D, Thanh HL, Antil S, Bertrand D, Corringer PJ, Changeux JP, et al. Functional determinants by which snake and cone snail toxins block the α7 neuronal nicotinic acetylcholine receptors. J Physiol Paris 1998;92:107-11.

[10] Antil-Delbeke S, Gaillard C, Tamiya T, Corringer PJ, Changeux JP, Servent D, et al. Molecular determinants by which a long chain toxin from snake venom interacts with the neuronal α7-nicotinic acetylcholine receptor. J Biol Chem 2000;275:29594-601.

[11] Grant GA, Luetje CW, Summers R, Xu XL. Differential roles for disulfide bonds in the structural integrity and biological activity of κ-bungarotoxin, a neuronal nicotinic acetylcholine receptor antagonist. Biochemistry 1998;37:12166-71.

[12] Lyukmanova EN, Shenkarev ZO, Schulga AA, Ermolyuk YS, Mordvintsev DY, Utkin YN, et al. Bacterial expression, NMR, and electrophysiology analysis of chimeric short/long-chain α-neurotoxins acting on neuronal nicotinic receptors. J Biol Chem 2007;282:24784-91.

[13] Broad AJ, Sutherland SK, Coulter AR. The lethality in mice of dangerous Australian and other snake venom. Toxicon 1979;17:661-4.

[14] Fairley NH, Splatt B. Venom yields in Australian poisonous snakes. Med J Aust 1929;1:336-48.

[15] Sutherland SK, Tibballs J. Genus *Acanthophis*, death adders. In: Australian Animal Toxins: The Creatures, Their Toxins and Care of the Poisoned Patient. Melbourne: Oxford University Press, 2001. p. 160-6.

[16] Mebs D, Samejima Y. Purification, from Australian elapid venoms, and properties of phospholipases A which cause myoglobinuria in mice. Toxicon 1980;18:443-54.

[17] Wickramaratna JC, Fry BG, Hodgson WC. Species-dependent variations in the *in vitro* myotoxicity of death adder (*Acanthophis*) venoms. Toxicol Sci 2003;74:352-60.

[18] Blacklow B, Escoubas P, Nicholson GM. Characterisation of the heterotrimeric presynaptic phospholipase A_2 neurotoxin complex from the venom of the common death adder (*Acanthophis antarcticus*). Biochem Pharmacol 2010;80:277-87.

[19] Kim HS, Tamiya N. The amino acid sequence and position of the free thiol group of a short-chain neurotoxin from common-death-adder (*Acanthophis antarcticus*) venom. Biochem J 1981;199:211-8.

[20] Sheumack DD, Howden ME, Spence I. Isolation and partial characterisation of a lethal neurotoxin from the venom of the Australian death adder (*Acanthophis antarcticus*). Toxicon 1979;17:609-16.

[21] Kim HS, Tamiya N. Isolation, properties and amino acid sequence of a long-chain neurotoxin, Acanthophis antarcticus b, from the venom of an Australian snake (the common death adder, *Acanthophis antarcticus*). Biochem J 1981;193:899-906.

[22] Sheumack DD, Spence I, Tyler MI, Howden ME. The complete amino acid sequence of a post-synaptic neurotoxin isolated from the venom of the Australian death adder snake *Acanthophis antarcticus*. Comp Biochem Physiol B 1990;95:45-50.

[23] Tyler MI, Retson-Yip KV, Gibson MK, Barnett DW, Howe E, Stöcklin R, et al. Isolation and amino acid sequence of a new long-chain neurotoxin with two chromatographic isoforms (Aa el and Ae e2) from the venom of the Australian death adder (*Acanthophis antarcticus*). Toxicon 1997;35:555-62.

[24] King GF, Gentz MC, Escoubas P, Nicholson GM. A rational nomenclature for naming peptide toxins from spiders and other venomous animals. Toxicon 2008;52:264-76.

[25] Chippaux JP, Williams V, White J. Snake venom variability: methods of study, results and interpretation. Toxicon 1991;29:1279-303.

[26] Blacklow B, Konstantakopoulos N, Hodgson WC, Nicholson GM. Presence of presynaptic neurotoxin complexes in the venoms of Australo-Papuan death adders (*Acanthophis* spp.). Toxicon 2010;55:1171-80.

[27] Ginsborg BL, Warriner J. The isolated chick biventer cervicis nerve-muscle preparation. Brit J Pharmacol Chemother 1960;15:410-1.

[28] Whiteaker P, Davies AR, Marks MJ, Blagbrough IS, Potter BV, Wolstenholme AJ, et al. An autoradiographic study of the distribution of binding sites for the novel α7-selective nicotinic radioligand [^{3}H]-methyllycaconitine in the mouse brain. Eur J Neurosci 1999;11:2689-96.

[29] Davies AR, Hardick DJ, Blagbrough IS, Potter BV, Wolstenholme AJ, Wonnacott S. Characterisation of the binding of [^{3}H]methyllycaconitine: a new radioligand for labelling α7-type neuronal nicotinic acetylcholine receptors. Neuropharmacology 1999;38:679-90.

[30] Christopoulos A, Coles P, Lay L, Lew MJ, Angus JA. Pharmacological analysis of cannabinoid receptor activity in the rat vas deferens. Br J Pharmacol 2001;132:1281-91.

[31] Christopoulos A, Parsons AM, Lew MJ, El-Fakahany EE. The assessment of antagonist potency under conditions of transient response kinetics. Eur J Pharmacol 1999;382:217-27.

[32] Arunlakshana O, Schild HO. Some quantitative uses of drug antagonists. Br J Pharmacol Chemother 1959;14:48-58.

[33] Lew MJ, Angus JA. Analysis of competitive agonist-antagonist interactions by nonlinear regression. Trends Pharmacol Sci 1995;16:328-37.

[34] Cheng Y, Prusoff W. Relationship between inhibition constant (K_I) and the concentration of an inhibitor which causes 50% inhibition (IC_{50}) of an enzymatic reaction. Biochem Pharmacol 1973;22:3099-108.

[35] Fry BG, Wickramaratna JC, Jones A, Alewood P, Hodgson WC. Species and regional variations in the effectiveness of antivenom against the in vitro neurotoxicity of death adder (*Acanthophis*) venoms. Toxicol Appl Pharmacol 2001;175:140-8.

[36] Hodgson WC, Wickramaratna JC. *In vitro* neuromuscular activity of snake venoms. Clin Exp Pharmacol Physiol 2002;29:807-14.

[37] Wickramaratna JC, Hodgson WC. A pharmacological examination of venoms from three species of death adder (*Acanthophis antarcticus*, *Acanthophis praelongus* and *Acanthophis pyrrhus*). Toxicon 2001;39:209-16.

[38] Fry BG, Wickramaratna JC, Hodgson WC, Alewood P, Kini RM, Ho H, et al. Electrospray liquid chromatography/mass spectrometry fingerprinting of *Acanthophis* (death adder) venoms: taxonomic and toxinological implications. Rapid Comm Mass Spectrom 2002;16:600-8.

[39] Lumsden NG, Fry BG, Ventura S, Kini RM, Hodgson WC. Pharmacological characterisation of a neurotoxin from the venom of *Boiga dendrophila* (mangrove catsnake). Toxicon 2005;45:329-34.

[40] Kuruppu S, Reeve S, Smith AI, Hodgson WC. Isolation and pharmacological characterisation of papuantoxin-1, a postsynaptic neurotoxin from the venom of the Papuan black snake (*Pseudechis papuanus*). Biochem Pharmacol 2005;70:794-800.

[41] Tan LC, Kuruppu S, Smith AI, Reeve S, Hodgson WC. Isolation and pharmacological characterisation of hostoxin-1, a postsynaptic neurotoxin from the venom of the Stephen's banded snake (*Hoplocephalus stephensi*). Neuropharmacology 2006;51:782-8.

[42] Kornhauser R, Hart AJ, Reeve S, Smith AI, Fry BG, Hodgson WC. Variations in the pharmacological profile of post-synaptic neurotoxins isolated from the venoms of the Papuan (*Oxyuranus scutellatus canni*) and coastal (*Oxyuranus scutellatus scutellatus*) taipans. Neurotoxicology 2010;31:239-43.

[43] Wickramaratna J, Fry B, Loiacono R, Aguilar M, Alewood P, Hodgson W. Isolation and characterization at cholinergic nicotinic receptors of a neurotoxin from the venom of the *Acanthophis* sp. Seram death adder. Biochemical Pharmacology 2004;68:383-94.

[44] Lee C, Pharmacological Institute CoM. Chemistry and Pharmacol. of polypeptide toxins in snake venoms. Annu Rev Pharmacol 1972;12:265-86.

[45] Gunja N, Ling M, Dowsett R, Murray L, Isbister GK. Antivenom and neostigmine failure in death adder envenoming. Clin Toxicol 2007;45:389.

[46] Lomazzo E, Macarthur L, Yasuda RP, Wolfe BB, Kellar KJ. Quantitative analysis of the heteromeric neuronal nicotinic receptors in the rat hippocampus. J Neurochem 2010;in press.

[47] Antil S, Servent D, Ménez A. Variability among the sites by which curaremimetic toxins bind to *Torpedo* acetylcholine receptor, as revealed by identification of the functional residues of α-cobratoxin. J Biol Chem 1999;274:34851-8.

[48] Ducancel F, Merienne K, Fromen-Romano C, Trémeau O, Pillet L, Drevet P, et al. Mimicry between receptors and antibodies. Identification of snake toxin determinants recognized by the acetylcholine receptor and an acetylcholine receptor-mimicking monoclonal antibody. J Biol Chem 1996;271:31345-53.

[49] Pillet L, Trémeau O, Ducancel F, Drevet P, Zinn-Justin S, Pinkasfeld S, et al. Genetic engineering of snake toxins. Role of invariant residues in the structural and functional properties of a curaremimetic toxin, as probed by site-directed mutagenesis. J Biol Chem 1993;268:909-16.

[50] Trémeau O, Lemaire C, Drevet P, Pinkasfeld S, Ducancel F, Boulain JC, et al. Genetic engineering of snake toxins. The functional site of erabutoxin a, as delineated by site-directed mutagenesis, includes variant residues. J Biol Chem 1995;270:9362-9.

[51] Lukas RJ, Morimoto H, Hanley MR, Bennett EL. Radiolabeled α-bungarotoxin derivatives: kinetic interaction with nicotinic acetylcholine receptors. Biochemistry 1981;20:7373-8.

[52] Wickramaratna JC. A pharmacological characterisation of death adder (*Acanthophis* spp.) venoms and toxins. PhD dissertation, Department of Pharmacology, Monash University, Australia 2003.

[53] Ishikawa Y, Ménez A, Hori H, Yoshida H, Tamiya N. Structure of snake toxins and their affinity to the acetylcholine receptor of fish electric organ. Toxicon 1977;15:477-88.

[54] Martin BM, Chibber BA, Maelicke A. The sites of neurotoxicity in α-cobratoxin. J Biol Chem 1983;258:8714-22.

[55] Weber M, Changeux JP. Binding of *Naja nigricollis* (^{3}H)α-toxin to membrane fragments from *Electrophorus* and *Torpedo* electric organs. I. Binding of the tritiated α-neurotoxin in the absence of effector. Mol Pharmacol 1974;10:1-14.

[56] Clarke C, Kuruppu S, Reeve S, Ian Smith A, Hodgson WC. Oxylepitoxin-1, a reversible neurotoxin from the venom of the inland taipan (*Oxyuranus microlepidotus*). Peptides 2006;27:2655-60.

[57] Wolf KM, Ciarleglio A, Chiappinelli VA. κ-Bungarotoxin: binding of a neuronal nicotinic receptor antagonist to chick optic lobe and skeletal muscle. Brain Res 1988;439:249-58.

[58] Loring RH, Andrews D, Lane W, Zigmond RE. Amino acid sequence of toxin F, a snake venom toxin that blocks neuronal nicotinic receptors. Brain Res 1986;385:30-7.

[59] Fry BG, Lumsden NG, Wuster W, Wickramaratna JC, Hodgson WC, Kini RM. Isolation of a neurotoxin (α-colubritoxin) from a nonvenomous colubrid: evidence for early origin of venom in snakes. Journal of Molecular Evolution 2003;57:446-52.

[60] Lumsden NG, Banerjee Y, Kini RM, Kuruppu S, Hodgson WC. Isolation and characterization of rufoxin, a novel protein exhibiting neurotoxicity from venom of the psammophiine, *Rhamphiophis oxyrhynchus* (Rufous beaked snake). Neuropharmacology 2007;52:1065-70.